Organic Process Research & Development **2009**, *13*, 991–998

Selective Hydrogenation of 2-Methyl-3-butyne-2-ol in a Wall-Coated Capillary Microreactor with a $Pd_{25}Zn_{75}/TiO_2$ Catalyst

Evgeny V. Rebrov,*[,†] Ekaterina A. Klinger,[†] Angel Berenguer-Murcia,[‡,⊥] Esther M. Sulman,[§] and Jaap C. Schouten[†]

Department of Chemical Engineering and Chemistry, Eindhoven University of Technology, P.O. Box 513, 5600 MB Eindhoven, The Netherlands, Department of Chemistry, Cambridge University, Lensfield Road, CB2 1EW Cambridge, U.K., and Tver Technical University, A. Nikitin Street, 22, Tver 170026, Russia

Abstract:

Continuous flow capillary microreactors with embedded monometallic (Pd) or bimetallic ($Pd_{25}Zn_{75}$) catalysts have been tested in the selective hydrogenation of alkyne reagents. The catalysts were prepared in two steps. At first, polymer-stabilized metal nanoparticles (either Pd or $Pd_{25}Zn_{75}$) were prepared by the reduction by solvent method. Then, a solution of colloidal nanoparticles with a desired concentration was added into a titania sol, which was destabilized by solvent evaporation during dip-coating of the inner wall of a fused silica capillary with an internal diameter of 250 μm. The wall-coated microreactors were tested in the hydrogenation of 2-methyl-3-butyne-2-ol (0.011−0.45 M solution in methanol) in the 328−337 K temperature range. The highest selectivity towards the alkene product of 90% was obtained at 99.9% conversion on the $Pd_{25}Zn_{75}/TiO_2$ catalyst. The selectivity was further increased to 97% by addition of pyridine into the reactant solution. No deactivation of the wall-coated catalysts was observed during one month of continuous operation at 333 K.

Introduction

During the last two decades, significant developments in the field of miniaturized systems, so-called microfluidics or lab-on-a-chip technologies, have been achieved and applied widely to diverse areas, such as catalysis,[1,2] fine chemicals synthesis,[3] polymerization,[4] and sensors.[5] In fine chemicals synthesis, these microreaction systems have found a wide range of applications in different chemical reactions in what is currently referred to as process intensification, which is directly aimed at improving the performance of existing processes. The synthesis of a large number of fine chemicals, particularly in the field of fragrance chemistry and pharmaceuticals, involves selective hydrogenation as a critical step. In these gas−liquid−solid reactions, the overall production rate is often limited by interphase mass transfer. To overcome this deficiency, multiphase reactions can be performed in microchannels or microcapillaries with a catalytic coating deposited on the channel wall. To perform hydrogenations in a microreactor and to avoid mass- and/or heat-transport limitations, both titania and silica thin films with embedded nanostructured catalysts have been developed in our laboratory.[1,6,7] They consist of an open mesoporous structure of a support with significant open porosity (usually 30−50%) in which the active material is dispersed.

Scheme 1. **Possible transformations of 2-methyl-3-butyne-2-ol**

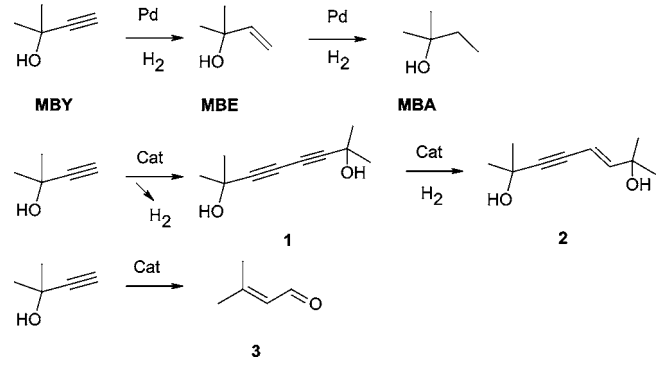

The selective hydrogenation of acetylene alcohols is an important step in the synthesis of fine chemicals, viz. vitamins A and E. Supported Pd catalysts are known to be very efficient for the hydrogenation of long-chain acetylene alcohols to ethylene alcohols. However, under several reaction conditions a number of side products can be formed (Scheme 1). Thus, under nitrogen atmosphere, oxidative dimerization dominates, and 2-methyl-3-butyn-2-ol (MBY) is converted over a Pd catalyst into 2,7-dimethyl-3,5-octadiyne-2,7-diol (**1**) which can further be hydrogenated to 2,7-dimethyl-5-octen-3-yne-2,7-diol (**2**).[8] Isomerization of MBY into prenal can be achieved in the presence of mixtures of titanium alkoxides, copper (I) chloride, and carboxylic acids.[9] A commonly used catalyst for the

* Corresponding author. E-mail: e.rebrov@tue.nl. Phone: +31 40 2472850.
† Eindhoven University of Technology.
‡ Cambridge University.
§ Tver Technical University.
⊥ Present address: University of Alicante, Departamento de Química Inorgánica, Ap. 99 - 03080, Alicante, Spain.

(1) Rebrov, E. V.; Berenguer-Murcia, A.; Skelton, H. E.; Johnson, B. F. G.; Wheatley, A. E. H.; Schouten, J. C. *Lab Chip* **2009**, *9*, 503–506.
(2) Kobayashi, J.; Mori, Y.; Okamoto, K.; Akiyama, R.; Ueno, M.; Kitamori, T.; Kobayashi, Sh. *Science* **2004**, *304*, 1305–1308.
(3) Kawaguchi, T.; Miyata, H.; Ataka, K.; Mae, K.; Yoshida, J.-I. *Angew. Chem.* **2005**, *44*, 2413–2416.
(4) Hessel, V.; Serra, C.; Löwe, H.; Hadziioannou, G. *Chem.-Ing.-Tech.* **2005**, *77*, 1693–1714.
(5) Wirnsberger, G.; Scott, B. J.; Stucky, G. D. *Chem. Commun.* **2001**, 119–120.
(6) Rebrov, E. V.; Berenguer-Murcia, A.; Johnson, B. F. G.; Schouten, J. C. *Catal. Today* **2008**, *138*, 210–215.
(7) Muraza, O.; Rebrov, E. V.; Khimyak, T.; Johnson, B. F. G.; Kooyman, P. J.; Lafont, U.; de Croon, M. H. J. M.; Schouten, J. C. *Chem. Eng. J.* **2008**, *135S*, S99–S103.
(8) Trofimov, B. A.; Sukhov, B. G.; Nosyreva, V. V.; Mal'kina, A. G.; Aleksandrova, G. P.; Grishchenko, L. A. *Dokl. Chem.* **2007**, *417*, 261–263.
(9) Lorber, C. Y.; Youinou, M.-T.; Kress, J.; Osborn, J. A. *Polyhedron* **2000**, *19* (14), 1693–1698.

10.1021/op900085b CCC: $40.75
Published on Web 06/01/2009

semihydrogenation of alkynes is a commercial Lindlar catalyst, calcium carbonate-supported palladium, modified by the addition of lead and, often, organic bases (e.g., quinoline) to improve selectivity.[10]

To explain the activity/selectivity behavior of Pd catalysts in the hydrogenation of alkynes, the specificity of the interaction of the catalytic centers with the carbon−carbon multiple bonds of the reagents and the electronic and morphological properties of the metal particles were considered.[11] A high selectivity to the alkene is related to an increased Pd electron density that leads to a decreased alkene adsorption. A higher selectivity to the alkene was achieved by employing electron-donor compounds, such as N-bases (quinoline, pyridine, and ammonia) or by the addition of electron-donor compounds (Pb, Zn) to the Pd nanoparticles.

It is possible to change the performance of a metal by tailoring the particle size[12] and the stoichiometry,[13] although the latter has not been thoroughly investigated. By changing the metal ratio in a bimetallic nanoparticle, different arrangements of the surface atoms can be obtained. The type and relative amount of these surface atoms will determine the catalytic behavior of the nanoparticle, which should be optimized for obtaining the highest activity and selectivity possible. Understanding the relationship between the stoichiometry of bimetallic nanoparticles and their activity/selectivity is of significant importance in assisting the development of new catalytic processes in microstructured reactors.

Herein we present the use of a continuous capillary microreactor with mesoporous titania thin films containing either Pd or bimetallic $Pd_{25}Zn_{75}$ nanoparticles for MBY hydrogenation. The nanoparticles with an average size of 2.5 nm were embedded in the titania support during sol−gel synthesis following previously reported methodology.[1,6] The effect of the 2-methyl-3-butyne-2-ol concentration was studied in the range from 0.011 to 0.45 M, the hydrogen partial pressure in the range from 0.30 to 0.80, and the reaction temperature between 328 and 337 K. The results are compared with the hydrogenation over $Pd_{25}Zn_{75}/TiO_2$/Si plates in a stirred reactor operating under a hydrogen pressure of 5 bar.

Results and Discussion

Optimization of Reaction Parameters. Table 1 summarizes the characteristics of the studied catalysts, while the reactor and process parameters are listed in Table 2. The main reaction products are 2-methyl-3-buten-2-ol (MBE) and 2-methyl-3-butan-2-ol (MBA). At low hydrogen partial pressure, significant amounts of the C_{10}-dimer (**1**) are produced. The adduct (**2**) is not observed during the present experiments. The supposed side product, prenal (**3**), is not observed−probably due to the absence of oxygen donors which are required to form a titanium propargyl-oxo complex.[9] The effect of the MBY concentration on the reaction rate was examined on the Pd/TiO_2 catalyst using three different concentrations (0.01, 0.20, and 0.45 M). Figure 1 shows the reaction rate as a function of the liquid flow rate in the microchannel. The initial concentration of MBY does not influence the selectivity to MBE nor the content of the byproduct formed. Within the whole range of MBY concentrations studied, the selectivity to MBE attains 96.5% at an MBY conversion below 20%, and the fraction of MBY transformed to byproducts amounts to 3.5%. This dependence of the reaction rate on the MBY concentration is in line with the zero reaction order in MBY. An addition of Zn at a Pd/Zn molar ratio of 1/3 considerably improves the selectivity to the semihydrogenated product (MBE) at high MBY conversion (Figure 2). The MBE selectivity is controlled by the ratio of the kinetic constants of the first and second hydrogenation steps as well as by the MBY

Table 1. **Characteristics of Pd/TiO_2 and $Pd_{25}Zn_{75}/TiO_2$ catalysts**

	Pd/TiO_2	$Pd_{25}Zn_{75}/TiO_2$
titania thickness, nm	105	110
titania apparent density[a], g/cm^3	2.13	2.13
coating weight in the reactor, mg	0.878	0.919
Pd loading, wt %	1.00	0.36
Zn loading, wt %	−	0.64
Pd/Zn molar ratio, -	−	0.33
mean metal particle average size[b], nm	2.5	2.5
Pd dispersion[c]	0.40	0.40

[a] Calculated from the film porosity. [b] Size of nanoparticles in the colloidal solution. [c] Estimated from the mean particle size.

Table 2. **Microreactor and process characteristics**

length, m	10
internal diameter, mm	0.250
catalyst loading, kg_{TiO2}/m^3	1.8
liquid flow range, mL /min	0.002−0.014
gas flow range, mL/min (STP)	0.60−1.00
Re_L, -	0.6−5.0
Re_G, -	1.1−1.8
H_2 partial pressure[a], -	0.3−1.0
liquid hold-up, -	0.21−0.33
pressure at the outlet, bar	1.0
pressure drop over the reactor, bar	1.2−2.7

[a] Nitrogen was used as a balance.

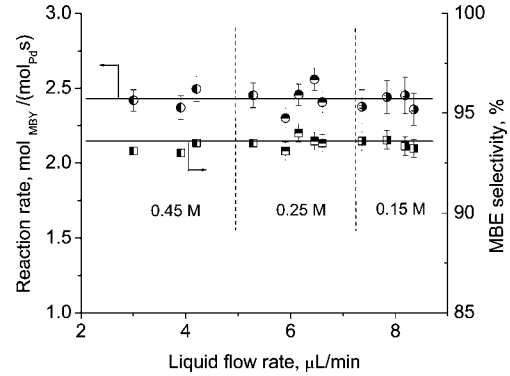

Figure 1. **Effect of initial concentration of 2-methyl-3-butyne-2-ol (MBY) on its hydrogenation rate and selectivity towards MBE formation over the $Pd_{25}Zn_{75}/TiO_2$ catalyst at 333 K. The initial concentration of MBY was varied between 0.011 and 0.15 M, while the liquid flow rate was varied between 9.0 and 2.3 μL/min to provide a conversion below 15%. The hydrogen flow was fixed at 0.9 mL/min (STP).**

(10) Lindlar, H.; Dubuis, R. *Org. Synth.* **1966**, *46*, 89–92.
(11) Molnar, A.; Sarkany, A.; Varga, M. *J. Mol. Catal. A: Chem.* **2001**, *173*, 185–221.
(12) Silvestre-Albero, J.; Rupprechter, G.; Freund, H. J. *J. Catal.* **2006**, *240*, 58–65.
(13) Aramendia, M. A.; Borau, V.; Jimenez, C.; Marinas, J. M.; Sempere, M. E.; Urbano, F. J. *Appl. Catal.* **1990**, *63*, 375–389.

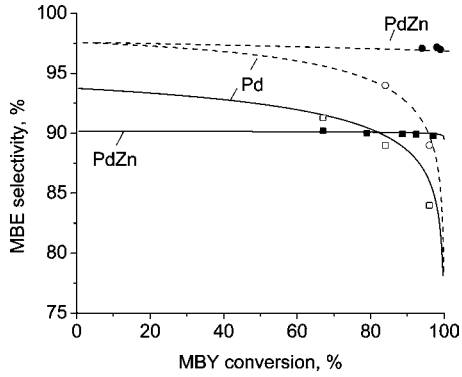

Figure 2. **Selectivity to MBE as a function of MBY conversion over Pd/TiO_2 (open symbols) and $Pd_{25}Zn_{75}/TiO_2$ (closed symbols) catalysts in the absence (solid lines and square symbols) and in the presence of pyridine (0.1 M, dashed lines and circle symbols) in the initial solution. Lines represent the kinetic model. Symbols represent experimental data in the capillary microreactor. Temperature: 333 K.**

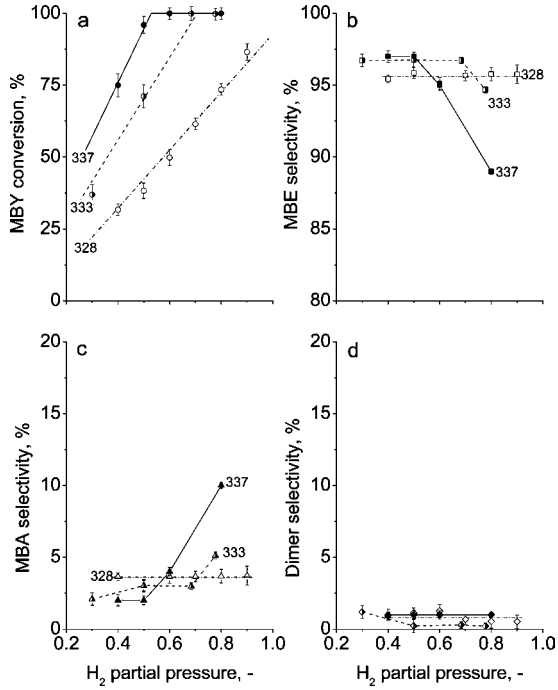

Figure 3. **(a) MBY conversion and (b−d) selectivity to MBY (b), MBA (c), and C_{10}-dimer (d) over $Pd_{25}Zn_{75}/TiO_2$ catalyst as a function of hydrogen partial pressure at different temperatures. Experimental data are given with symbols. The lines are drawn as a guide for the eye. Solid lines and closed symbols represent 337 K; dashed lines and half-open symbols: 333 K; and dash/dotted lines and open symbols: 328 K. The total gas flow rate (hydrogen and nitrogen) was kept constant at 1.0 mL/min (STP). Liquid flow: 9.2 μL/min.**

and MBE adsorption constants. The origin of this high MBE selectivity of the $Pd_{25}Zn_{75}/TiO_2$ catalyst will be discussed in the following section based on the reaction kinetics.

A systematic study of the effects of the reaction temperature and the hydrogen partial pressure was performed over $Pd_{25}Zn_{75}/TiO_2$ (Figure 3). A linear dependence of the reaction rate on the hydrogen partial pressure up to a conversion of 95% demonstrated that the reaction is first order in hydrogen, and zero order in MBY, in the whole range of temperatures studied (Figure 3a). The curves at temperatures below 328 K are not shown in Figure 3 as a lower selectivity to MBE was observed at these conditions. The apparent activation energy of the MBY hydrogenation is 64 kJ/mol. This was calculated from an Arrhenius plot (not shown) derived from the temperature dependence of the MBY hydrogenation reaction rate shown in Figure 3. The selectivity to MBE increases with temperature; however, the influence of the temperature on the selectivity was found to be far less decisive than that of the pressure (Figure 3b). The maximum MBE yield was observed at a temperature of 337 K. However, fast catalyst deactivation was observed close to the boiling point of methanol at 337 K; therefore, the maximum temperature was fixed at 333 K during the kinetic study. After reaching full MBY conversion, further increase in hydrogen pressure resulted in a higher selectivity to MBA (Figure 3c) while the selectivity to the C_{10}-dimers remained unchanged and did not exceed 2% (Figure 3d).

It should be mentioned that at a liquid flow rate of, e.g., 5 μL/min, it takes 100 min to collect enough sample for the GC analysis (4−6 sampling points per day with 100−110 points per month for each catalyst, the flow being fed to the reactor overnight as well). Therefore, the time-on-stream of each catalyst was more than one month during which no deactivation was observed at a temperature of 333 K with a few experimental runs performed at lower temperatures.

An important characteristic of the catalytic material is the amount of metal leaching during exposition to the fluid. This undesirable effect can occur in three different ways, as pointed out in ref 14: (i) very low metal leaching (under the limit of detection of an adequately sensible analytical technique), practically negligible; (ii) significant leaching of catalytically active metal species; (iii) significant leaching of inactive metal species. The last two cases can also include total or partial readsorption of the metal species on the support surface downstream of the reactor channel. It appeared from this study that colloidal nanoparticles deposited on mesoporous titania oxide are entirely leaching free (case (i)) due to their embedding into the titania network. In an accompanying study (not shown here as this is beyond the scope of this paper), we have demonstrated that the Ti^{3+} sites were formed after calcination of the mesoporous titania films containing metal nanoparticles at 573 K. A strong metal support interaction (SMSI) in the supported nanostuctured catalysts prevents metal leaching from the mesoporous support.

The rate of C_{10}-dimer formation is, in general, an order of magnitude lower than that of MBA, at least in the concentration range studied; therefore, the concentration curves of the C_{10}-dimer are not presented in several figures as its concentration is below or just above the detection limit. The MBY conversion decreases with increasing liquid flow rate (Figure 4). In the range of gas and liquid velocities applied, an annular two-phase flow was realized in the microchannel, such that the gas flowed along the centre of the tube, while the liquid flowed along the channel walls as a liquid film. The liquid hold-up and the liquid residence time were calculated according to the Lockhart−Martinelli−Chisholm correlation. The MBY conversion as a

(14) Sheldon, R. A.; Wallau, M.; Arends, I. W. C. E.; Schuchardt, U. *Acc. Chem. Res.* **1998**, *31*, 485–493.

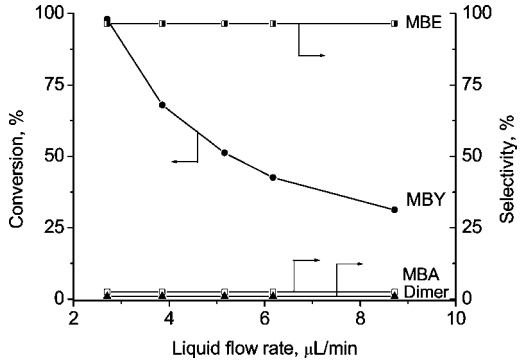

Figure 4. **MBY conversion and selectivity to major products over $Pd_{25}Zn_{75}/TiO_2$ catalyst as a function of liquid flow rate. Hydrogen flow rate: 0.9 mL/min (STP). Temperature: 333 K.**

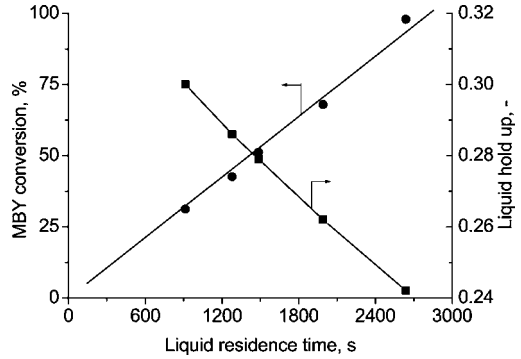

Figure 5. **MBY conversion and liquid hold-up over $Pd_{25}Zn_{75}/TiO_2$ catalyst as a function of liquid residence time.**

function of the liquid residence time gives a straight line passing through the origin (Figure 5). This sustains the correctness of the applied approach for the calculation of the liquid residence time.

The effect of the liquid residence time, the presence of Zn, and the addition of pyridine in the initial solution is investigated by comparing the Pd/TiO_2 and $Pd_{25}Zn_{75}/TiO_2$ catalysts. A nitrogen base (NB) is typically used in the concentrations corresponding to a NB/Pd molar ratio in the range from 4 to 1500 and an NB/reactant molar ratio of 0.1−1.[13] Typical concentration curves of the alkyne, alkene and alkane are shown in Figure 6. The reaction proceeds through two well-separated stages clearly observable on the MBE curve. In the initial stage lasting until ~96% conversion on the Pd catalyst and almost until 99.5% conversion on the $Pd_{25}Zn_{75}$ catalyst, the semihydrogenation of MBY to MBE (C≡C to C=C) is the main reaction. Then, the second stage started. It can be seen that the second stage proceeds much faster on the Pd catalyst as compared with the $Pd_{25}Zn_{75}$ catalyst. An addition of pyridine at a pyridine/MBY ratio of 0.1 decreases the MBY hydrogenation rate, and it results in a wider maximum on the MBE concentration curve. It should be pointed out that in the presence of pyridine the initial MBY concentration was reduced by 4.5 times to achieve full MBY conversion (see Figure 6a, right *y*-axis). On the $Pd_{25}Zn_{75}$ in the absence of pyridine, the first and second hydrogenation steps have approximately the same reaction rate as it can be seen from the slope of the corresponding concentration curves in Figure 6b. The formation of C_{10}-dimers is suppressed. It appears that the insertion of Zn into

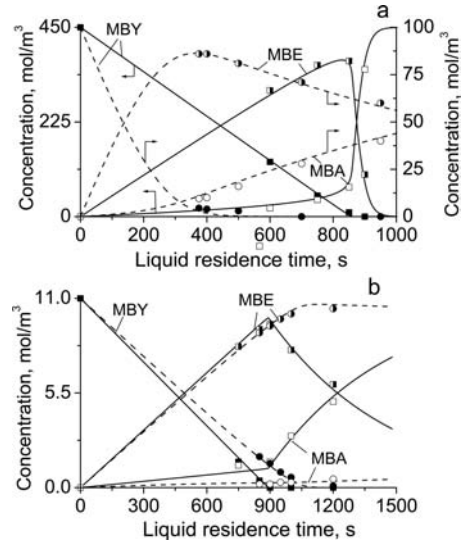

Figure 6. **Product distribution in the absence of pyridine (solid lines and square symbols) and in the presence of pyridine (dashed lines and circle symbols, pyridine/MBY molar ratio: 0.1) in the reactant solution over (a) Pd/TiO_2, (b) $Pd_{25}Zn_{75}/TiO_2$ catalysts as a function of the liquid residence time in the microreactor. Lines represent the concentration profiles obtained with the kinetic model. Experimental data for MBY are given with closed symbols; for MBE with half-open symbols; and for MBA with open symbols. Temperature: 333 K. Hydrogen flow: 0.9 mL/min (STP).**

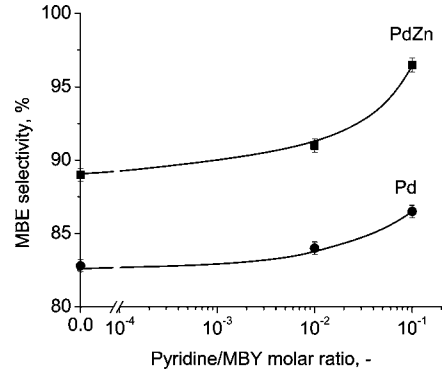

Figure 7. **MBE selectivity at the maximum yield of MBE as a function of the pyridine/MBY molar ratio over Pd/TiO_2 and $Pd_{25}Zn_{75}/TiO_2$ catalyst. Lines represent the kinetic model. Symbols represent experimental data. Temperature: 333 K.**

the Pd nanoparticles drastically decreases the number of multiple palladium sites responsible for the dissociative adsorption of MBY. This pathway is reported to lead to the formation of C_{10}-dimers and further hydrogenation of C_{10}-dimers adsorbed on the Pd sites.[8,15] As opposed to the Pd curves, the addition of pyridine at a pyridine/MBY ratio of 0.1 does not change the rate of MBY hydrogenation while it almost completely suppresses the second hydrogenation step (Figure 6b). In this case equal initial concentrations of MBY were used. In Figure 7 the concentration dependence of the selectivity is presented by decreasing the amount of modifier in the reactant stream.

(15) Leviness, S.; Nair, V.; Weiss, A. H.; Schay, Z.; Guczi, L. *J. Mol. Catal.* **1984**, *25*, 131–140.

Scheme 2. **Kinetic Model**

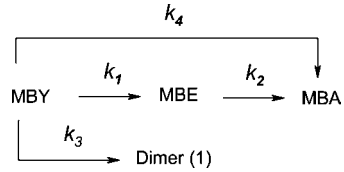

Between experiments with different concentrations of pyridine, an experiment was always performed without addition of pyridine.

In analogy to Figure 2, a higher selectivity was always accompanied by a substantial decreasing MBY hydrogenation rate on the Pd catalyst, while the hydrogenation rate remained practically unchanged on the $Pd_{25}Zn_{75}$ (not shown in Figure 7). Both catalysts have a similar nanoparticle size of ca. 2.5 nm, while the Pd content in the $Pd_{25}Zn_{75}/TiO_2$ catalyst was 4 times lower than that in the Pd/TiO_2 catalyst. However, the initial reaction rate at 333 K in terms of TOF was 2.4 s^{-1} on the Pd/TiO_2 versus 0.15 s^{-1} on the $Pd_{25}Zn_{75}/TiO_2$. In this estimation it was assumed that Pd and Zn are equally distributed throughout the bimetallic nanoparticles, or in other words there is no rearrangement of metals during the calcination step. The reaction rate is comparable to that reported for the unsupported Pd nanoparticles.[16] The reaction rates in terms of TOF of ~2 s^{-1} are typical for kinetically limited systems. The maximum value of the overall mass transfer coefficient (k_{ov}) in the capillary microreactor is 0.01 $m_L^3\ m_R^{-3}\ s^{-1}$. This value is rather low as compared with bulk mass transfer-limited systems (k_{ov} is of the order of 0.1 $m_L^3\ m_R^{-3}\ s^{-1}$) and hardly varies with varying hydrodynamics (there being no difference in k_{ov} between slug and annular flow). This justifies the conclusion that interface mass transfer is not the rate determining factor in these capillary reactors and intrinsic kinetics is observed. The TOF value observed on $Pd_{25}Zn_{75}/TiO_2$ was comparable with that observed on the commercial Lindlar catalyst (5 wt % $Pd/CaCO_3$) but more then 3 times lower than that observed on a spent Pd/ZnO catalyst at 308 K.[17]

Kinetic Model. From the study of the hydrogenation of acetylene alcohols carried out by various authors the occurrence of three possible pathways can be inferred. Pathway 1 takes place through the associative adsorption of MBY and yields the semihydrogenated product, MBE (Scheme 2). Pathway 2 takes place through the associative adsorption of MBE and yields the fully hydrogenated product (MBA). Pathway 3 involves the dissociative adsorption of MBY on neighboring Pd sites and results in the formation of C_{10}-dimers. Many catalysts are deactivated as a result of the absorption of the C_{10}-dimers close to the Pd surface and the consequent blocking of the active sites.[13] As it is shown in the previous section, mass transfer effects on the reaction rate are negligible compared to the overall reaction rate. Therefore, kinetic equations can be applied without including mass transfer in the modeling. Taking into consideration the weak hydrogen adsorption on Pd,[18] as well as that the K_DC_D term is much smaller than at least one of the following terms: K_YC_Y, K_EC_E, K_AC_A, or K_DC_D in the whole range of experimental conditions studied, the reaction rate equations can be written as eqs 1−3 (see Scheme 2):

$$r_1 = \frac{k_1 K_Y C_Y C_{H_2}}{1 + K_Y C_Y + K_E C_E + K_{P_1} C_P} \quad (1)$$

$$r_2 = \frac{k_2 K_E C_E C_{H_2}}{1 + K_Y C_Y + K_E C_E + K_A C_A + K_{P_1} C_P} \quad (2)$$

$$r_3 = \frac{k_3 K_Y^2 C_Y^2}{(1 + K_Y C_Y + K_E C_E + K_{P_1} C_P)^2} \quad (3)$$

Where k_n is the rate constant for reaction n; K_Y, K_E, K_A, K_D, and K_{P_1} are the adsorption constants, and C_Y, C_E, C_A, C_D, and C_P are the concentrations of alkyne, alkene, alkane, dimers and pyridine, respectively. The hydrogen concentration (C_{H_2} = 16.5 mol/m^3) was calculated from existing solubility data.[19] To model the reaction satisfactory for the selectivity as well, it is necessary to add a direct alkyne to alkane hydrogenation step (Pathway 4). Pathway 4 involves the reaction of MBY with hydrogen adsorbed on the catalyst to form an intermediate species responsible for the formation of the alkane and thus detracting from the MBE selectivity.[13]

The effect of pyridine on the selectivity can not be described with only one type of pyridine adsorption site. On the basis of previously published results, an increase of the selectivity in the presence of organic bases can be explained by a preferential adsorption of the additive over alkenol on the selective sites[20] and strong adsorption on the nonselective sites.[21,22] Assuming that step 4 takes place on the nonselective sites, two different adsorption constants of pyridine (on selective and nonselective sites) are introduced in the model, while other constants are assumed to be the same on both sites to limit the number of fitted parameters (eq 4).

$$r_4 = \frac{k_4 K_Y C_Y C_{H_2}}{1 + K_Y C_Y + K_E C_E + K_A C_A + K_{P_2} C_P} \quad (4)$$

A similar step occurred on the nonselective sites that were included in the mechanism of acetylene hydrogenation.[23,24] The authors concluded that the relative significance of the two paths and, therefore, the selectivity can be controlled by the catalyst and reaction conditions.

Fitting the model containing these equations to a number of experiments in the presence of pyridine resulted in a value for the equilibrium constants for adsorption of pyridine on the selective and the nonselective sites, K_{P1}, K_{P2}, of 100 and 960

(16) Domínguez-Domínguez, S.; Berenguer-Murcia, A.; Pradhan, B. K.; Cazorla-Amoŕ; os, D.; Linares-Solano, Á. *J. Catal.* **2006**, *243*, 74–81.
(17) Semagina, N.; Grasemann, M.; Xanthopoulos, N.; Renken, A.; Kiwi-Minsker, L. *J. Catal.* **2007**, *251*, 213–222.
(18) Singh, U. K.; Vannice, M. A. *J. Catal.* **2000**, *191*, 165–180.
(19) Descamps, C.; Coquelet, C.; Bouallou, C.; Richon, D. *Thermochim. Acta* **2005**, *430*, 1–7.
(20) Nijhuis, T. A.; van Koten, G.; Kapteijn, F.; Moulijn, J. A. *Catal. Today* **2003**, *79−80*, 315–321.
(21) Tschan, R.; Schubert, M. M.; Baiker, A.; Bonrath, W.; Rotgerink, L. H. *Catal. Lett.* **2001**, *75*, 31–36.
(22) Siegel, S.; Hawkins, J. A. *J. Org. Chem.* **1986**, *51*, 1638–1640.
(23) Bos, A. N. R.; Westerterp, K. R. *Chem. Eng. Process.* **1993**, *32*, 1–8.
(24) Al-Ammar, A. S.; Webb, G. *J. Chem. Soc., Faraday Trans.* **1979**, *75*, 1900–1911.

Table 3. **Parameter values for the kinetic model in the hydrogenation of MBY on Pd/TiO_2 and $Pd_{25}Zn_{75}/TiO_2$ catalysts at 333 K**

catalyst	Pd/TiO_2	confidence interval	$Pd_{25}Zn_{75}/TiO_2$	confidence interval
k_1, $m^3/mol/s$	1.8×10^{-1}	± 0.02	1.1×10^{-2}	$\pm 1.3 \times 10^{-3}$
k_2, $m^3/mol/s$	4.0	± 0.5	9.3×10^{-2}	± 0.012
k_3, s^{-1}	2.3×10^{-4}	fixed	1.0×10^{-5}	fixed
k_4, $m^3/mol/s$	1.1×10^{-2}	± 0.002	1.2×10^{-3} (2.6×10^{-3})[a]	$\pm 2.0 \times 10^{-4}$
K_Y, m^3/mol	20	± 2.8	2.1×10^{2}	± 25
K_E, m^3/mol	3.5×10^{-2}	± 0.006	2.3×10^{-2}	± 0.002
K_A, m^3/mol	1.3×10^{-2}	fixed	1.3×10^{-2}	fixed
K_{P_1}, m^3/mol	1.0×10^{2}	± 12	1.0×10^{2}	± 12
K_{P_2}, m^3/mol	9.6×10^{2}	± 80	9.6×10^{2}	± 80
Pd concentration, mol/m^3	1.7×10^{-1}		6.1×10^{-2} (2.1×10^{-4})	
k_1/k_2, −	0.045		0.12	
K_Y/K_E, −	570		9100	

[a] Values in the brackets are given for the batch reactor.

m^3/mol, respectively (Table 3). Apparently pyridine adsorbs on Pd even more strongly than the alkyne, which is the explanation of the reduction in the overall reaction rate. On the contrary, the absorption constant of MBY on the $Pd_{25}Zn_{75}$ catalyst more than twice exceeds that of pyridine, therefore its addition up to the 0.1 pyridine/MBY ratio does not influence the hydrogenation rate.

Due to the higher adsorption enthalpy of the alkynes, ($K_Y/K_E = 570$ and 9100 on Pd and $Pd_{25}Zn_{75}$, respectively), the surface coverage of alkyne exceeds that of alkene until 99 and 99.9% conversion of alkyne on the Pd and $Pd_{25}Zn_{75}$ catalysts, respectively. This means that the alkyne either displaces the alkene from the surface or blocks its readsorption. As a consequence, an alkene is not hydrogenated in the presence of an alkyne on the selective sites, while it undergoes ready hydrogenation in the absence of the alkyne.

The K_Y/K_E ratio of 570 observed in this study is close to that obtained in the hydrogenation of 1-hexyne over a 3 wt % Pd/C catalyst where a ratio of 133 was reported.[25] In the same study, a k_1/k_2 ratio of 0.12 was found which is more than 2 times higher than that in the present work.[25] An even higher k_1/k_2 ratio of 2.3 is reported in a recent study on MBY hydrogenation over a Pd/ZnO catalyst deposited on sintered metal fibers, while the K_Y/K_E ratio of 950 is almost 2 times higher than that in the present study.[17] These results suggest that the kinetic constants for the Pd/TiO_2 thin films are in the range of earlier reported values for supported Pd catalysts.

As the MBY conversion increases from 5 to 95%, the $(r_1 - r_2)/(r_1 + 2r_3 + r_4)$ ratio, which determines the selectivity to MBE, drops from 0.94 to 0.52 over the Pd/TiO_2 catalyst, while it remains virtually the same (0.90 and 0.89) over the $Pd_{25}Zn_{75}/TiO_2$ catalyst (see Figure 2). In the presence of pyridine, this ratio drops from 0.98 to 0.56 over the Pd/TiO_2 catalyst, while over the $Pd_{25}Zn_{75}/TiO_2$ it drops only from 0.98 to 0.96. This is mainly due to the fact that the adsorption constant K_Y is an order of magnitude larger on the $Pd_{25}Zn_{75}/TiO_2$ compared to that on the Pd/TiO_2 catalyst.

An additional experimental run was performed in the batch reactor to compare the results with those in the capillary microreactor with the $Pd_{25}Zn_{75}$ catalyst (Figure 8). The experimental curves for MBY, MBE, and MBA can be modeled with

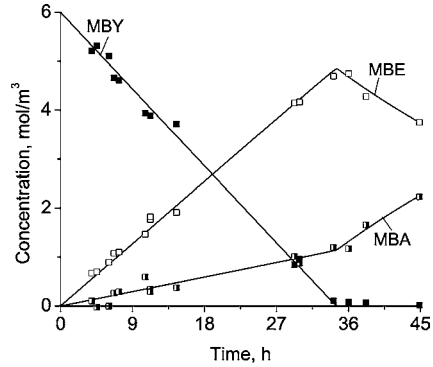

Figure 8. **Product distribution in hydrogenation of MBY over $Pd_{25}Zn_{75}/TiO_2$ catalyst as a function of the reaction time in the batch reactor. Lines represent the kinetic model. Symbols represent experimental data. Temperature: 333 K. Pressure: 5 bar. Catalyst weight: 0.98 mg.**

the same set of kinetic and adsorption constants as those in the microreactor. The only significant difference was obtained in the value of the rate constant of the direct hydrogenation on the nonselective sites in accordance with a slightly lower selectivity to MBE of 81% obtained in the batch reactor. A lower selectivity can be explained by the different preparation procedures of the thin films (dip-coating in the microreactor vs spin-coating in the batch reactor) which might result in a different concentration of the nonselective sites.

Table 4 summarizes the best results obtained on the Pd and $Pd_{25}Zn_{75}$ catalysts. These results allow to conclude that wall-coated capillary microreactors can be used as an efficient tool in fine chemicals synthesis. The selectivity towards the semi-hydrogenated product in the microreactor is even higher than that observed in the batch reactor, while there is no need for a subsequent catalyst separation step. It seems to be possible to further improve the productivity in the hydrogenation of acetylene alcohols by changing the stoichiometry of the $Pd_{25}Zn_{75}$ nanoparticles embedded in the mesoporous titania framework by increasing the Pd/Zn ratio in the nanoparticles.

An important parameter in industrial hydrogenation is the catalyst cost per kilogram of product produced. The costs of the in-house-made thin films with the embedded nanoparticles are between 3 and 4 Euros per gram of support for the Zn/TiO_2 and pure Pd/TiO_2 thin films, respectively. These costs do not take into account manpower and electricity costs required for their preparation. In general, the price of the in-house-made

(25) Dobrovolná, Z.; Kačer, P.; Červeny, L. *J. Mol. Catal. A: Chem.* **1998**, *130*, 279–284.

Table 4. **Comparison of maximum MBE selectivity over Pd/TiO_2 and $Pd_{25}Zn_{75}/TiO_2$ catalysts**

catalyst	reactor	additives	MBY conversion, %	MBE selectivity, %
$Pd_{25}Zn_{75}/TiO_2$	batch	−	96.0	81.1
Pd/TiO_2	microreactor	−	96.0	83.0
$Pd_{25}Zn_{75}/TiO_2$	microreactor	−	99.9	89.5
$Pd_{25}Zn_{75}/TiO_2$	microreactor	pyridine	99.9	97.0

[a] Conversion from the range of 96−100% at which maximum selectivity was obtained.

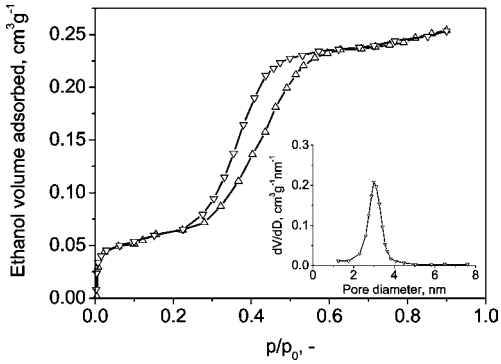

Figure 9. **Ethanol adsorption−desorption isotherms on the mesoporous titania support (without nanoparticles) at 287 K and the corresponding pore size distribution.**

catalytic coatings remains competitive with the current price of the commercial Lindlar catalyst produced at a similar scale (about 4−5 Euros per gram according to Sigma-Aldrich[26]). It should be mentioned however, that the weight of the catalytic coating in a 10 m capillary microreactor is about 0.9 mg. This makes the catalyst costs less than 1% of the microreactor hardware (capillary, mixing unit, and fittings). Of course the contribution from the microreactor hardware will further decrease during scale-up of a single capillary to a multiple capillary microreactor assembly, consisting of several hundreds or thousands of capillaries running in parallel.

Conclusions

Novel capillary microreactors that were wall-coated with mesoporous titania thin films containing embedded Pd or $Pd_{25}Zn_{75}$ (with a molar Pd/Zn ratio of 0.33) nanoparticles have been tested in the hydrogenation of 2-methyl-3-butyne-2-ol in methanol by hydrogen. The highest selectivity to the semihydrogenated product was obtained at 333 K with pure hydrogen. Increasing the nitrogen fraction in the gas phase resulted in a substantial formation of 2,7-dimethyl-3,5-octadiyne-2,7-diol via oxidated dimerization. The Pd/TiO_2 catalyst demonstrated an order of magnitude higher hydrogenation reaction rate compared to the commercial Lindlar catalyst and gave an alkene selectivity of 89% at 96% alkyne conversion at 3 bar hydrogen pressure in the presence of pyridine. The selectivity was considerably improved towards 97% at 99.9% conversion over the $Pd_{25}Zn_{75}/TiO_2$ catalyst, also in the presence of pyridine. The subsequent MBE hydrogenation step and the C_{10}-dimer formation were suppressed. However, in the latter case, the reaction rate dropped by a factor of 16 compared to that with the Pd/TiO_2 catalyst. Further fine-tuning of the nanoparticle composition by increasing the Pd/Zn molar ratio can improve the catalyst performance. The challenge here is to find an optimum Pd/Zn ratio which would still provide a high activity of the Pd catalyst while maintaining a high selectivity observed on the $Pd_{25}Zn_{75}$ catalyst.

Experimental Section

Microreactors. The incorporation of the metal nanoparticles in the mesoporous titania thin films has been done by addition of a fraction of the colloidal solution containing either Pd or $Pd_{25}Zn_{75}$ nanoparticles to the initial solution containing the titania precursor, the surfactant, and the solvent. This approach was successfully applied in a previous study for the synthesis of catalytic thin films containing Au nanoparticles.[1] After ageing, the solution was used to dip-coat the internal surface of a fused silica capillary with an internal diameter of 250 μm and a length of 10 m. The characteristics of the Pd/TiO_2 and $Pd_{25}Zn_{75}/TiO_2$ catalysts are listed in Table 1. In the kinetic tests, a mixture of 2-methyl-3-butyn-2-ol (MBY) in methanol (0.011−0.45 M with or without addition of pyridine) was mixed with a hydrogen/nitrogen mixture. The gas and liquid were mixed in a T-mixer, the internal diameters of the inlet and outlet tubes were 250 μm. The gas was fed at an angle of 90° with respect to the liquid flow. The liquid flow was varied between 2 and 12 μL/min and the H_2/N_2 flow between 0.250 and 1.0 mL/min (STP).

Batch Reactor. Silicon substrates with a cross section of 9.8 × 9.8 mm^2 and with a thickness of 0.5 mm were used. The films were deposited on both sides of the substrates by spin-coating at 1500 rpm at a relative humidity (RH) of 80%. The as-deposited films were kept at 80% RH for 24 h; then the temperature was increased to 573 K under a residual pressure of 10 mbar at a heating rate of 1 K/min followed by a dwelling interval of 4 h at 573 K. Ten $Pd_{25}Zn_{75}/TiO_2/Si$ samples were placed in an autoclave reactor with a total volume of 270 mL and were in situ reduced at 523 K at a H_2 pressure of 10 bar for 1 h. Then, the reactor was cooled to room temperature. A 0.011 M solution of MBY in methanol (130 mL) was deoxygenated and transferred into the reactor. The hydrogenation reaction was performed at 333 K and 5 bar hydrogen pressure under intensive stirring at 1500 rpm. The analysis of the reaction mixture (2-methyl-3-butyn-

(26) http://www.sigmaaldrich.com.

(27) Protasova, L. N.; Rebrov, E. V.; Ismagilov, Z. R.; Schouten, J. C. *Microporous Mesoporous Mater.* **2009**, doi:10.1016/j.micromeso.2009.04.006.

(28) Haverkamp, V.; Hessel, V.; Löwe, H.; Menges, G.; Warnier, M. J. F.; Rebrov, E. V.; De Croon, M. H. J. M.; Schouten, J. C.; Liauw, M. A. *Chem. Eng. Technol.* **2006**, *29*, 1015–1026.

2-ol, 2-methyl-3-buten-2-ol, 2-methylbutan-2-ol, 2,7-dimethyl-3,5-octadiyne-2,7-diol) was performed off-line with a Varian CP-3800 gas chromatograph equipped with a CP-Sil 5 CB capillary column (diameter: 1 mm, length: 30 m) and an FID detector. Each compound was quantified by authentic reference substances. To calculate standard deviations, four samples were taken for analysis.

Characterization. The mesopore volume (porosity) and the pore size distribution of the films deposited on the flat substrates were determined by ellipsometric porosimetry (EP) from desorption isotherms of ethanol at 287 K using the Bruggerman effective media approximation (BEMA) and the modified Deriaguin−Broekhoff−de Boer (BDdB) theory.[27] The mean pore size of mesoporous titania prepared without addition of metal nanoparticles in the synthesis solution was 3.0 nm (see Figure 9). The bulk composition of the nanoparticles was measured by emission spectroscopy (ICP-OES in a Perkin-Elmer Optima 4300) after an aliquot of the colloids was dissolved in HNO_3. The samples were treated with 2 mL of HNO_3 diluted with ultrapure water and analyzed for their metal content.

(29) Chisholm, D. J. *Heat Mass Transfer* **1967**, *10*, 1767–1778.
(30) Lu, P.; Teranishi, T.; Asakura, K.; Miyake, M.; Toshima, N. *J. Phys. Chem. B* **1999**, *103*, 9673–9682.

Acknowledgment

We thank Prof. D. Yu. Murzin from Abo Akademi University for his comments on the manuscript. The financial support by the British Council-NWO Partnership Programme in Science, Projects PPS 888 and 894, is gratefully acknowledged.

Supporting Information Available

Calculation of the liquid hold-up and residence time in the microreactor; mass balances in the batch reactor; preparation of Pd and $Pd_{25}Zn_{75}$ bimetallic nanoparticles; preparation of a mesoporous thin film with embedded nanoparticles; Figure S1: TEM images of the prepared $Pd_{25}Zn_{75}$ colloidal nanoparticles; Figure S2: particle size distribution of $Pd_{25}Zn_{75}$ nanoparticles. This material is available free of charge via the Internet at http://pubs.acs.org.

Received for review April 7, 2009.

OP900085B